RB

# GSI

GSI-Preprint-95-71
NOVEMBER 1995

X FROM $^{20}$Mg TO THE $^{100}$Sn REGION: BETA-DECAY STUDIES OF PROTON DRIP-LINE NUCLEI

Contribution to the Int. Nucl. Phys. Conf. (INPC '95), Bejing, P.R. of China, 1995;
Proc. to be published by World Scientific, Singapore

FROM $^{20}$Mg TO THE $^{100}$Sn REGION: EXPERIMENTAL TECHNIQUES FOR DECAY STUDIES OF PROTON DRIP-LINE NUCLEI

Contribution to the 2nd Int. Symp. on Heavy Ion Physics and Its Applications, (II SHIPA), Lanzhou, P.R. of China, 1995;
Proc. to be published by World Scientific, Singapore

E. ROECKL



Gesellschaft für Schwerionenforschung mbH
Postfach 11 05 52 · D-64220 Darmstadt · Germany

# FROM $^{20}$Mg TO THE $^{100}$Sn REGION: BETA–DECAY STUDIES OF PROTON DRIP–LINE NUCLEI

**Ernst Roeckl**
Gesellschaft für Schwerionenforschung,
Postfach 110552, D–64220 Darmstadt, Germany
E-mail: E.ROECKL@GSI.DE

ABSTRACT

The $\beta$–decays of $^{20}$Mg, $^{36}$Ca and $^{37}$Ca were investigated by using beam line spectrometers at GANIL, Caen, and GSI, Darmstadt. The results from these studies are presented together with those on decay properties of nuclei near $^{100}$Sn, investigated at the online mass separator of GSI. Emphasis is put on a comparison of the experimental Gamow–Teller strength with model predictions, a discussion of level assignments of interest to the astrophysical rp process, a determination of the solar neutrino capture cross-section of $^{37}$Cl, and a search for cluster radioactivity from $^{114}$Ba.

## 1 Introduction

During the last few years improvements in experimental techniques have permitted detailed studies of the $\beta$–decays of very proton–rich nuclei [1, 2]. Characterized by high energy release, these decays allow one to extract the Gamow–Teller (GT) strengths for transitions to a large range of excitation energies in the daughter nucleus and thus represent a valuable tool for testing the quality of model calculations. This holds, e.g., for the sd–shell nuclei $^{20}$Mg, $^{36}$Ca and $^{37}$Ca which have $Q_{EC}$ values of 10726(28), 10990(40), and 11639(22) keV [3], respectively. The latter two cases provide the additional possibility that the $\beta$–decay B(GT) strengths can be compared to the B(GT) function extracted from the (p,n) reactions on the N = 20 mirror nuclei for transitions into several final states. This is interesting as, under the assumption of isospin symmetry, the B(GT) functions for the $\beta$–decay of $^{37}$Ca and the $^{37}$Cl(p,n)$^{37}$Ar reaction as well as for the $\beta$–decay of $^{36}$Ca and the $^{36}$S(p,n)$^{36}$Cl reaction should be identical.

Among nulcei far from the $\beta$–stability line very neutron–deficient isotopes near the doubly–magic nucleus $^{100}$Sn (Z=N=50) have met considerable experimental and theoretical interest recently. Most of the experimental progress in this field has been achieved by in–beam spectroscopy or by studying (ground–state) decay properties, this report being focused on the second topic. In addition to effects such as the occurrence of iospin mixing (see, e. g., [4, 5, 6]) or proton halos (see, e. g., [7, 8]), the following features make the $^{100}$Sn region unique with respect to gaining new insight into nuclear-structure phenomena: Firstly, owing to the fact that protons and neutrons occupy identical ($g_{9/2}$) shell-model orbits, one may encounter superallowed $\alpha$ and cluster emission beyond $^{100}$Sn. Secondly, $\beta$-decay decay in this region is dominated by a fast (superallowed) $\pi g_{9/2} \rightarrow \nu g_{7/2}$ (or, for Z,N<50, also by a $\pi g_{9/2} \rightarrow \nu g_{9/2}$) GT transition. This dominance is expected to facilitate both the experiments, that are limited due to low source strengths, and the comparison with model predictions.

Most of the nuclei discussed in this paper lie very close to the proton drip line: If one considers neighbouring isotopes with one neutron less than $^{20}$Mg or $^{94}$Ag, for example, the corresponding nuclei either have a very small predicted proton separation energy ($660 \pm 550$ keV [3]) or are predicted by most of the current mass-formulae [9] to be proton-unbound, respectively.

The $\beta$-decays mentioned above are also of astrophysical interest. The A = 37 B(GT) function, for example, is needed for calibrating the measurement of the solar-neutrino flux by means of the $^{37}$Cl detector [10]. Furthermore, the study of the decay of $^{20}$Mg and $^{36}$Ca may yield information of levels in $^{20}$Na and $^{36}$K, that play an important role in the "break-out" reactions $^{19}$Ne(p,$\gamma$)$^{20}$Na and $^{35}$Ar(p,$\gamma$)$^{36}$K, respectively, of the astrophysical rp process [11, 12]. It has even been speculated that this nucleosynthesis process may extend up to heavy elements such as tin. In such a case, the decay properties measured for nuclei near $^{100}$Sn may allow one to test rp-process models which, e.g., predict a significant overproduction of $^{92}$Mo, $^{94}$Mo, $^{96}$Ru and $^{98}$Ru [13].

This report describes a detailed study of the $\beta$-delayed proton ($\beta p$) and $\gamma$-ray ($\beta\gamma$) emission of $^{20}$Mg, $^{36}$Ca and $^{37}$Ca, performed by means of the LISE3 facility at GANIL, Caen, and the projectile fragment separator FRS at GSI, Darmstadt, respectively. Moreover, recent experiments on neutron-deficient isotopes near $^{100}$Sn are presented, that were carried out at the isotope separator online (ISOL) of GSI. Emphasis is put on the physics results whereas details on the related experimental techniques are discussed elsewhere [14].

## 2 Beta-Decay of $^{20}$Mg

The investigation of the decay of $^{20}$Mg [15] at GANIL yielded an improved half-life value of $95 \pm 3$ ms and an improved decay scheme established on the basis of $\beta\gamma$, $\beta p$ and proton-$\gamma$ coincidence data. The resulting GT strength above excitation energies of 3 MeV is more fragmented than predicted by using the effective GT operator determined from the universal sd-shell interaction (USD model) [16]. For the astrophysically interesting 2645 keV level in $^{20}$Na, an upper limit of 0.1% was derived for the $\beta$-feeding, corresponding to a lower limit of 6.24 for the log ft value. Therefore, a $1^+$ assignment for this state is not very probable, even though it cannot be completely excluded [15].

# 3 Beta–Decay of $^{36}$Ca

Figure 1 compiles the new results obtained for the $^{36}$Ca decay [17] at GSI. The nonobservation of the astrophysically interseting 1890 keV state in $^{36}$K suggests that a $1^+$ assignment is excluded for this level (From a comparison with the analog level in the mirror nucleus $^{36}$Cl one would expect a $1^+$ or $2^+$ assignment). Two strong $\beta\gamma$–transitions to proton–bound states in $^{36}$K at 1112.8(4) and 1619.0(2) keV were observed, whereas six transitions to proton–unbound levels at 3370(29), 4289(8), 4457(33), 4687(37), 5947(47) and 6798(71) keV were identified in the $\beta p$–spectrum shown in figure 1c. The energy of the 3370(29) keV state represents a weighted mean of the new result of 3390(41) and the literature value of 3350(40) [18]. The energy of 4289(8) keV for the isobaric analog state (IAS) in $^{36}$K has been taken from the

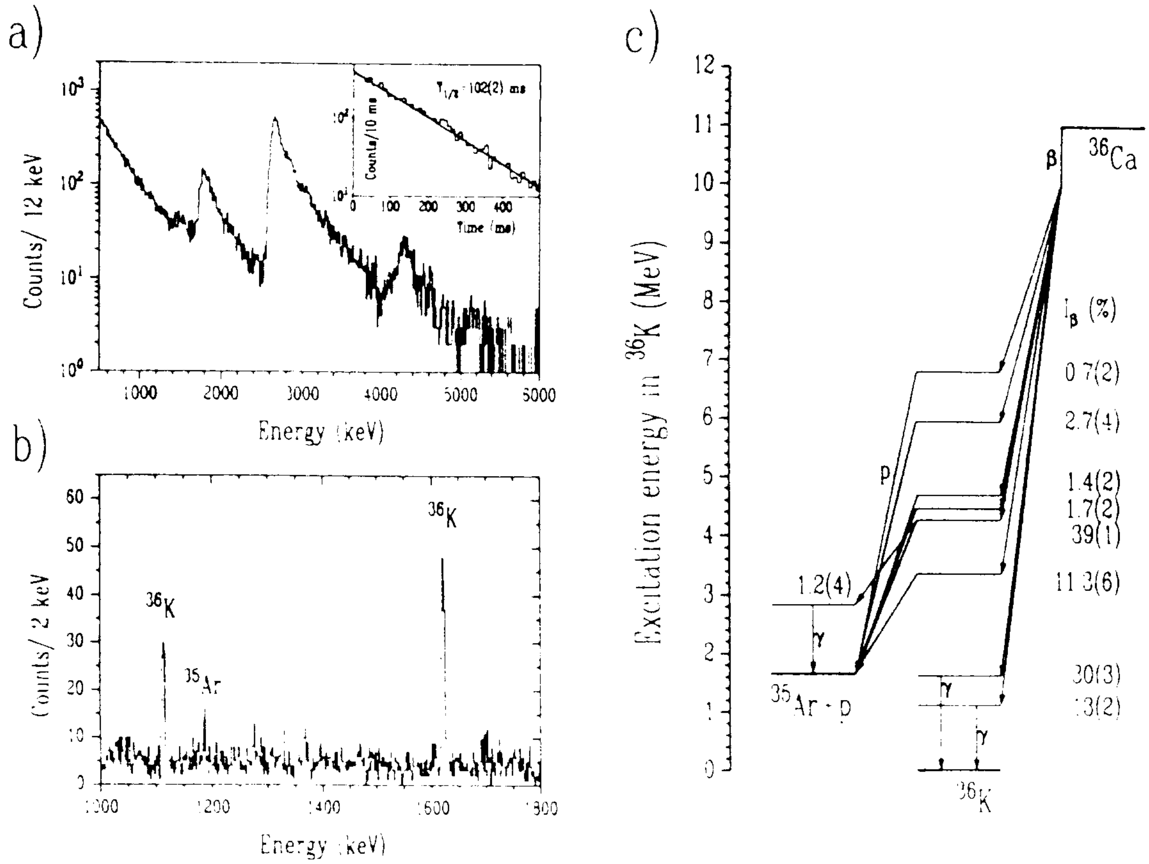


Figure 1: *Results obtained for the $\beta$-decay of $^{36}$Ca at GSI. a) proton spectrum (decay-time characteristics shown as inset), b) $\gamma$-spectrum in coincidence with $\beta$-rays in the implantation detector, and c) decay scheme ($I_\beta$ = branching ratio). The assignment for the $\gamma$ lines is given by indicating the nuclides in which the transition occurs. The weak $^{35}$Ar line originates from the $\beta$-decay of the implanted contaminant $^{35}$K and from the proton decay of the IAS in $^{36}$K to the first excited state in $^{35}$Ar.*

recent work of Garcia et al. [19] which agrees with the previous result of 4258(24) keV obtained by Äystö et al. [20] and the GSI value of 4287(39) keV. IAS in $^{36}$K decays mainly by proton emission to the $^{35}$Ar ground state ($p_0$) and with a weak branch to the first excited state of $^{35}$Ar ($p_1$). From the line intensities in the $\beta p$ spectrum a value of $\Gamma_{p_1}/\Gamma_{p_0} = 0.03(1)$ was extracted. The $^{36}$Ca half-life was measured to be $102 \pm 2$ ms (see inset in figure 1a). The resulting value for the Fermi strength in the $^{36}$Ca $\beta$-decay B(F) = 4.09(14) is consistent with the model-independent value B(F) = (Z − N) = 4 [16].

In comparison to theory, the B(GT) strength measured for the $\beta$-decay $^{36}$Ca and $^{37}$Ca (see below) is well reproduced up to about 4 MeV by USD model which, on the other hand, systematically underestimates the strength for transistions into highly excited final states [17, 21, 22] (see figure 2). The total B(GT) strength is better reproduced by applying the Chung-Wildenthal Hamiltonian [23] in the shell–

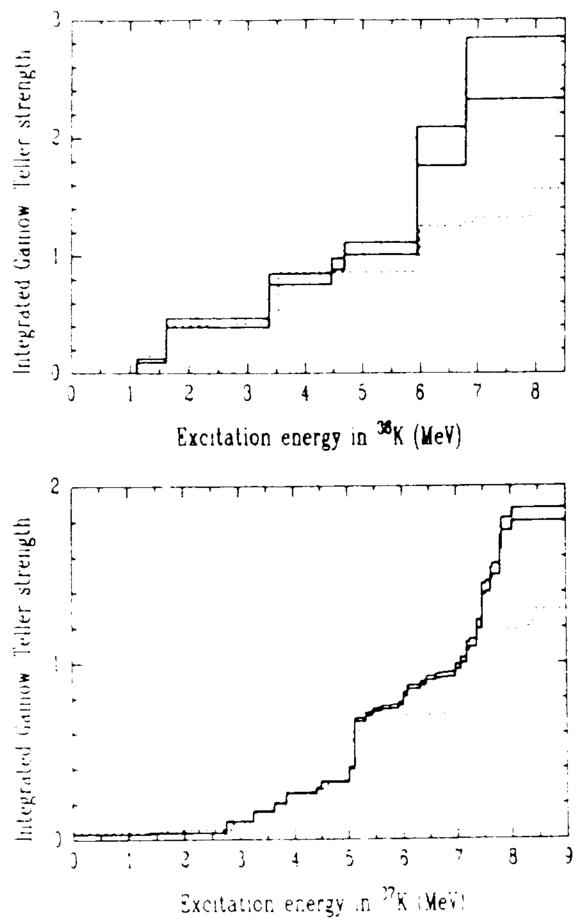


Figure 2: *Comparison of the summed B(GT) strength of $^{36}$Ca (upper panel) $^{37}$Ca (lower panel) from experiment (solid-line histograms) with the results of USD calculations (dashed-line histograms). For the experimental data the uncertainty due to one standard deviation is shown.*

model calculations. A similiar effect was observed for the $\beta$–decay of $^{38}$Ca [24]. The The discrepancy between $\beta$–decay strength and USD prediction has probably be to ascribed to the interactions rather than to the influence of intruder states [25].In this context, (p,n) experiments are important. However, the (p,n) data show some inconsistencies for the case of $^{37}$Ca, as will be discussed below, and are not available yet for the case of $^{36}$Ca. ($^{36}$S(p,n) measurements are apparently difficult due to low isotopic abundance of $^{36}$S.)

# 4 Beta–Decay of $^{37}$Ca

A previous high–resolution study of the $\beta$–delayed proton emission of $^{37}$Ca [26] revealed large discrepancies between the $\beta$–decay and the $^{37}$Cl(p,n)$^{37}$Ar reaction [27, 28] that cannot be ascribed to isospin asymmetries alone. Investigations of the $^{40}$Ca(p,$\alpha$)$^{37}$ [29] and $^{36}$Ar(p,$\gamma$)$^{37}$K [30] reactions showed that some proton–unbound states in $^{37}$K significantly decay also via $\gamma$–emission. The B(GT) asymmetries claimed for the A = 37 system might thus originate from the normalization of the $^{37}$Ca $\beta$–decay scheme used in [26], which was based on the assumption $\Gamma = \Gamma_p$ for all proton–unbound states in the daughter nucleus $^{37}$K fed by allowed $\beta$–decay of $^{37}$Ca.

Figure 3 shows the results on the decay of $^{37}$Ca, obtained at GSI recently [22]. In this experiment, the $\gamma$–deexcitation of the first three excited states of $^{37}$K fed by allowed $\beta$–decay of $^{37}$Ca was observed for the first time. They have excitation energies of 1370.9(2), 2750.4(2) and 3239.3(2) keV and receive a $\beta$–feeding of 2.1(1), 2.8(1) and 4.8(2) %, respectively. The values for the $\beta\gamma$– intensities have meanwhile been confirmed [31].

Combining the $\beta\gamma$ and $\beta p$ intensities measured at GSI, with the known [18] $\gamma$–deexcitation pattern of the 2750.4 keV state, values of $\Gamma_\gamma/\Gamma_p = 0.54(3)$ for this level and $\Gamma_\gamma/\Gamma_p = 22(2)$ for the 3239.3 keV state have been obtained. Furthermore, the known resonance strengths $\omega\gamma$ of the $^{36}$Ar(p,$\gamma$)$^{37}$K reaction of 0.208(30) eV [18] and 0.60(15) meV [30] for the states at 2750.4 keV and 3239.3 keV, respectively, together with the new $\Gamma_\gamma/\Gamma_p$ values allow one to deduce the partial widths and the corresponding mean lifetimes $\tau$ (see table 1). The value of $\tau = 2.2(2)$ fs for the 2750.4 keV state is consistent with the previously found upper limit $\tau < 3$ fs [18], while the new partial $\gamma$–decay widths $\Gamma_\gamma$ are considerably different from the known widths of the particle–bound (i.e. $\Gamma = \Gamma_\gamma$) mirror states in $^{37}$Ar [18]. The surprisingly domin–

Table 1: *Lifetimes and decay widths of excited states in $^{37}K$.*

| E/keV | $\Gamma_p$/eV | $\Gamma_\gamma$/eV | $\tau$/fs | $\Gamma(^{37}$Ar)/eV [18] |
|---|---|---|---|---|
| 2750.4 | 0.20(3) | 0.11(2) | 2.2(2) | 0.033(10) |
| 3239.3 | $2.1(6)\cdot 10^{-4}$ | $4.6(1.2)\times 10^{-3}$ | 140(40) | $8(1)\times 10^{-3}$ |

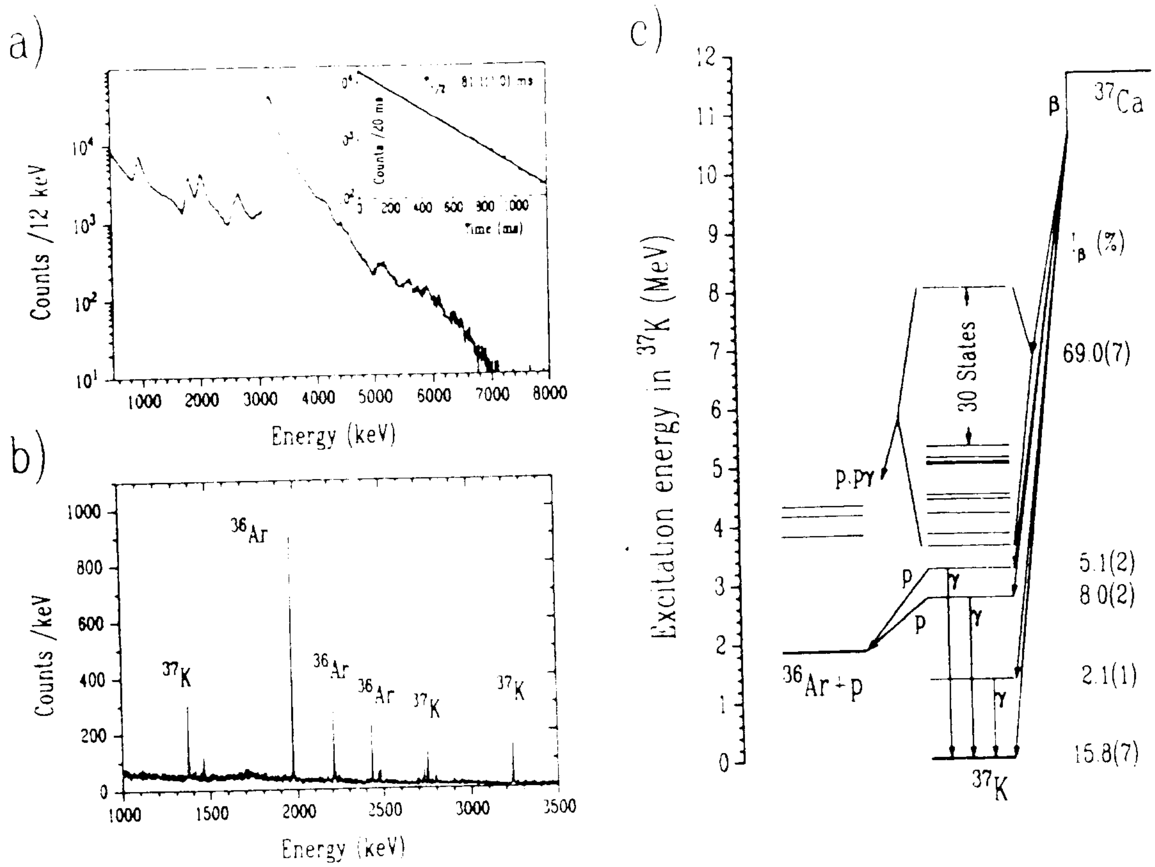


Figure 3: *Results obtained for the $\beta$-decay of $^{37}Ca$ at GSI. a) proton spectrum (decay-time characteristics shown as inset), b) $\gamma$-spectrum in coincidence with $\beta$-rays in the implantation detector, and c) decay scheme ($I_\beta$ = branching ratio). The assignment for the $\gamma$ lines is given by indicating the nuclides in which the transition occurs. The $^{36}Ar$ lines originate from the $\beta$-decay of the implanted contaminant $^{36}K$ and from the proton decay of excited states in $^{36}K$ to excited states in $^{36}Ar$. The branching ratio for the ground-state transition was obtained from $I_{GS} = 1 - \sum_i I^i_\beta$, $I_{GS}$ and $I^i_\beta$ being the decay branching ratios to the ground state and the level i in $^{37}K$, respectively.*

ating $\gamma$-decay of the 3239.3 keV state, which is unbound by more than 1.3 MeV, is due to an extremely suppressed proton-decay of this level (see table 1).

The half-life of $^{37}$Ca was redetermined to be $181.1 \pm 1.0$ ms (see inset in Figure 3a), this value being two standard deviations larger than the previously accepted result [18]. Including our delayed $\gamma$-ray intensities, the discrepancies between the B(GT) functions of the $^{37}$Ca decay and the $^{37}$Cl(p,n)$^{37}$Ar are drastically reduced (see table 2). Furthermore, the B(GT) value measured for the ground-state transition agrees very well with that of the $^{37}$Ar(EC)$^{37}$Cl mirror transition [16]. In addition to the above-mentioned comparison between experimental and calculated B(GT) values (see figure 2), the new results allow one to deduce evidence, at a level of 1.7 standard deviations, for an isospin-mixing amplitude between the IAS and the 5016

Table 2: *B(GT) values for low excitation energies in $^{37}K$. The values of the (p,n)-data [27] have been multiplied by $(g_A/g_V)^2 = (1.26)^2$ because of a different definition of B(GT). The (p,n)-data taken from [28] represent preliminary results.*

| $E_x(^{37}K)$/MeV | $\beta$-decay [22] | $\beta$-decay [26] | (p,n) [27] | (p,n) [28] |
|---|---|---|---|---|
| 0.0 | 0.048(2) | | 0.054(11) | |
| 1.3709 | 0.0126(6) | | < 0.014 | |
| 2.7504 | 0.102(3) | 0.067(4) | | 0.077(10) |
| 3.2393 | 0.087(4) | 0.0039(9) | | 0.136(15) |

keV state in $^{37}$K [22]. The neutrino-capture cross section for $^{37}$Cl, deduced from the new B(GT) and B(F) data to be $1.09(3)\times10^{-42}$ cm$^{-2}$, is consistent with the value that has so far been assumed for estimating, on the basis of standard solar-model calculations [32, 33, 26], the solar-neutrino rate of the $^{37}$Cl detector.

# 5 The Region around $^{100}$Sn

Even though the section of the chart of nuclides near $^{100}$Sn, which represents an ideal testing ground for the spherical shell-model, is occasionally considered to be a "well-known doubly magic region" [34], only some gross properties have been measured [35, 36, 37] for $^{100}$Sn so far, and the few-nucleon excitation states around the $^{100}$Sn core are also poorly known. The present experimental status on decay properties of Z≅N nuclei in the silver-to-barium region, displayed in Figure 4, is based almost exclusively on measurements performed by using beam-line spectrometers or isotope separators online (ISOL). In most of the ISOL experiments relevant here, the neutron-deficient isotopes of interest were produced by fusion-evaporation reactions such as $^{50}$Cr($^{58}$Ni,xpyn) and mass-separated as singly-charged 60 keV beams for subsequent decay studies. Figure 4 includes in particular recent and partly unpublished data on, e. g., $^{94}$Ag [38], the heaviest N=Z nucleus with known decay properties; the isotope identification obtained for $^{98}$In, $^{99}$In, $^{100}$Sn, $^{102}$Sn and $^{104}$Sb [35, 36]; $^{101}$Sn [39], the closest decay-spectroscopy approach to $^{100}$Sn achieved to date; the proton-radioactive nucleus $^{105}$Sb [40]; and the light barium isotopes [41, 42].

The decay of nuclear ground-states by the emission charged-particles allows one to identify rare nuclei, to determine their mass by "linking" the measured Q values to known masses [44], and to deduce information on the particle-emitting (ground) state and on the daughter states [38]. The region of neutron-deficient isotopes above tin is well suited for a discussion of the interplay between $\alpha$, proton and cluster radioactivities (see Figure 4). The existence of an island of $\alpha$ emission between $^{106}$Te and $^{114}$Cs is the most convincing experimental proof for the occurrence

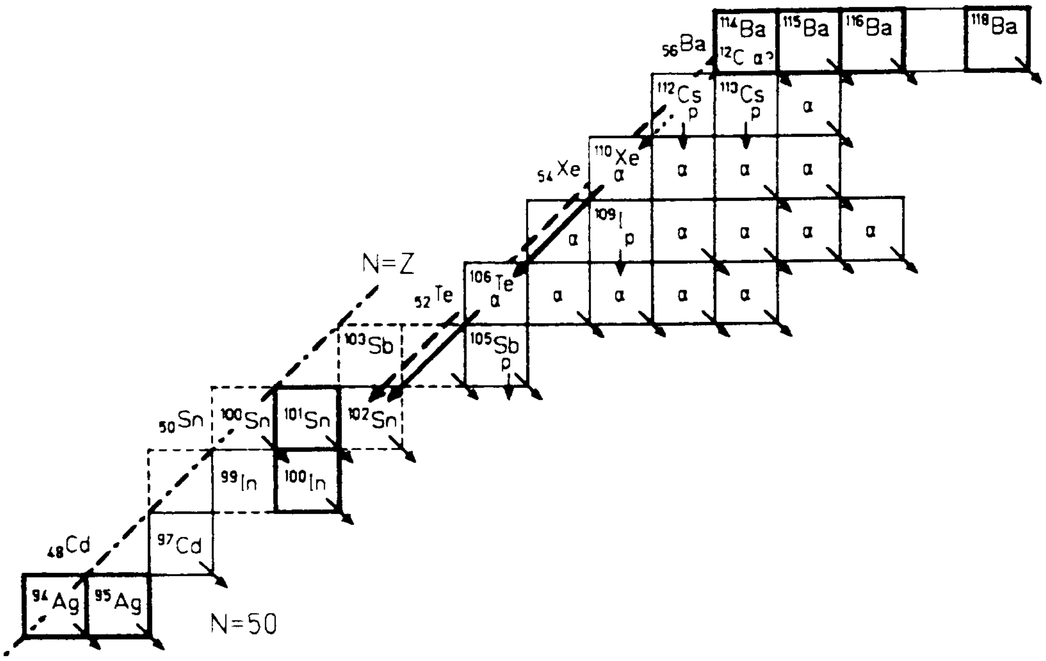


Figure 4: *Section of the chart of nuclides, showing the lightest known isotopes from silver to barium. Arrows indicate charged-particle and $\beta^+$/EC-decay modes, with "α" and "p" marking α and proton radioactive nuclei, respectively. Note in particular the three consecutive α-decays starting from $^{114}$Ba and the $^{12}$C-decay of this nucleus. New isotopes whose decay properties have recently been measured by using the GSI ISOL facility are marked by heavily outlined boxes. Dashed boxes indicate cases studied by means of beam-line spectrometers.*

of a shell closure at Z=50 and N=50: Similar to the conclusions drawn from the α decay data of the heaviest elements [44], it can be shown, with reference to predictions from macroscopic-microscopic mass formulae (see e.g. [34]), that the large measured $Q_\alpha$ values are almost entirely due to the shell effect (For N-Z=2 nuclei, for example, the $Q_\alpha$ value *decreases*, when going away from the valley of β-stability, from 4.32 MeV for $^{106}$Te to 3.88 MeV for $^{110}$Xe, whereas a macroscopic mass model [34] would predict an *increase* from approximately 1.1 to 1.4 MeV). Another interesting result is that the α widths measured in this region so far, namely those of $^{106}$Te and $^{110}$Xe, do *not* support the concept of superallowed α decay of these nuclei.

The double shell-closure at $^{100}$Sn gives also rise to two other ground-state decay modes involving charged-particle emission. One of them is proton radioactivity [45], experimentally identified for $^{105}$Sb [40], $^{109}$I, $^{112}$Cs [46], and $^{113}$Cs. It is interesting to note that the spectroscopic factor determined for the proton decay of $^{109}$I, $^{112}$Cs and $^{113}$Cs is below unity which is interpreted as reflecting different shape of mother and daughter nucleus [45]. Another exotic decay mode above $^{100}$Sn is the $^{12}$C decay of $^{114}$Ba. Recent measurements, performed by using the GSI ISOL facility, have allowed one to identify the new isotopes $^{114-116}$Ba and $^{118}$Ba, to study their decays [42], and to collect isotopically separated $^{114}$Ba atoms for a search for $\alpha$ and cluster radioactivity [41]. So far, the latter measurement has yielded only lower limits of $1.2\times10^2$ and $1.1\times10^3$ s for the partial $\alpha$ and $^{12}$C half-life, repectively, of $^{114}$Ba [41]. It is a challenge to try to improve these results with the aim of unambigiously identifying these disintegration modes of $^{114}$Ba.

The region near $^{100}$Sn was discussed so far with emphasis put on the direct emission of charged particles from nuclear ground states. However, this area of the chart of nuclides has also been subject of an intense programme of $\beta$-decay studies recently [38, 39, 41, 42, 47, 48, 49, 50, 51, 52]. As has already been mentioned, $\beta$-decay in this region of nuclei is dominated by a $\pi g_{9/2}\rightarrow\nu g_{7/2}$ (or, for Z,N<50, also by a $\pi g_{9/2}\rightarrow\nu g_{9/2}$) GT transition. Correspondingly, $\beta$ decay experiments allow one to investigate, even with low source strengths, the GT strength distribution and to compare it with model predictions. Recent shell-model calculations (see [52] and references therein) indicate that $^{100}$Sn decays almost exclusively by (superallowed) GT transition to the $1^+\{\pi g_{9/2}^{-1},\nu g_{7/2}\}$ GT resonance state in $^{100}$In, whereas neighbouring nuclei show in constrast a complex and broad distribution of the GT strength. In the following, some recent $\beta$-decay studies will be discussed, obtained by using the ISOL systems at CERN and at GSI, respectively. The measurements include $\beta$-delayed $\gamma$-rays for $^{100}$Ag, $^{98}$Cd, $^{103,104}$In and $^{105}$Sn as well as $\beta$-delayed protons for $^{94,95}$Ag, $^{100,102}$In and $^{101,103,105}$Sn.

The decay of *even-even* nuclei such as $^{98}$Cd [47] is characterized by the feeding of several $1^+$ levels in the odd-odd daughter nuclei instead of one $1^+\{\pi g_{9/2}^{-1},\nu g_{7/2}\}$ state as expected from the extreme single-particle shell model. The excitation-energy of the observed $1^+$ states ranges from 1.7 to 2.5 MeV in rough agreement with what is expected from shell-model considerations for the two-quasiparticle state. The splitting of the GT-strength has been interpreted as being due to residual $\pi g_{9/2}$-$\nu g_{7/2}$ interactions. Part of the GT strength is missed by the experiment because of the restricted decay-energy window and of the limited experimental sensitivity. Additional reduction is caused by core polarization effects in the parent nuclei. However, even when all calculated hindrance factors are taken into account, part of the GT-strength still seems to be missing when comparing the theoretical values to the experimental data of N=50 isotones. The question is whether the nuclear structure and the experimental limitations are understood well enough to assign at least part of this still missing strength to subnucleonic effects (For sd-shell nuclei, 2/3 of the quenching of the GT operator has been ascribed to higher-order configuration mixing and 1/3 to $\Delta$-admixtures [53]).

The decay of *even-odd* nuclei such as $^{101,103,105}$Sn [39, 50, 48] is expected to be governed by a resonance-like, but broad beta-strength function whose maximum, at an excitation energy of approximately 3.3 MeV in the odd-even daughter nuclei, might be ascribed to the coupling of an odd $d_{5/2}$ neutron to the GT pair $1^+\{\pi g_{9/2}^{-1},\nu g_{7/2}\}$. The calculated half-lives agree with the measured ones for $^{105,103}$Sn, whereas the value of 1.4 s, predicted for $^{101}$Sn, deviates somewhat from the experimental result of 3±1 s [39, 52] (see figure 5a). The observation that the predicted proton energy distribution is more narrow than the experimental one (see figure 5b) indicates that the GT strength is spread over more (comlicated) states than assumed in the calculation [52].

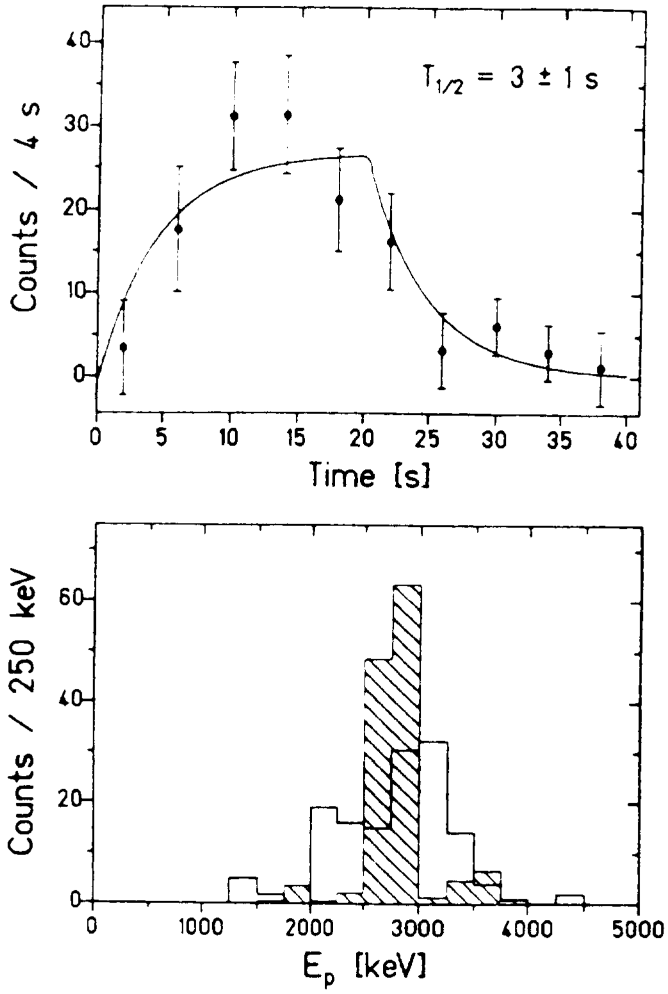


Figure 5: *a) Grow-in and decay time characteristic of the $\beta p$ decay of $^{101}Sn$, detected during consecutive 20 s intervals with the mass-101 beam switched on and off, respectively. The experimental data are given as circles, while the curve represents the best fit obtained by assuming one decay component. b) Comparison of the experimental $\beta p$ energy spectrum of $^{101}Sn$ (blank histogram) with the spectrum predicted by a shell-model calculation.*

In addition to high-resolution techniques for detecting positrons, X-rays as well as $\beta\gamma$- and $\beta$p radiation, a total-absorption $\gamma$-ray spectrometer was used to study the decay of the *odd-odd* nuclei near 100Sn, namely $^{100,102,104}$In [49] and $^{100}$Ag [51]. Here one expects the dominant population of a four-quasiparticle structure at an excitation energy of the order of 5 MeV in the final even-even nuclei, consisting of a GT pair $1^+\{\pi g_{9/2}^{-1}, \nu g_{7/2}\}$ from the respective core decay coupled to the spectator particles, i. e. the odd $d_{5/2}$-neutron and the odd $g_{9/2}$-proton. Indeed, results obtained for positrons, X-rays and $\beta$-delayed protons from the decay of $^{100,102}$In [49] (see figure 6) and $^{103,105}$Sn [50, 48] indicate such a dominant four-quasiparticle component of the strength distribution. This is qualitatively confirmed by the total absorption data measured for $^{100}$Ag [51] (see figure 7) and $^{104}$In [49] (Note that in figure 7 experimental data for $^{100}$Ag are compared to calculations for $^{98}$Ag).

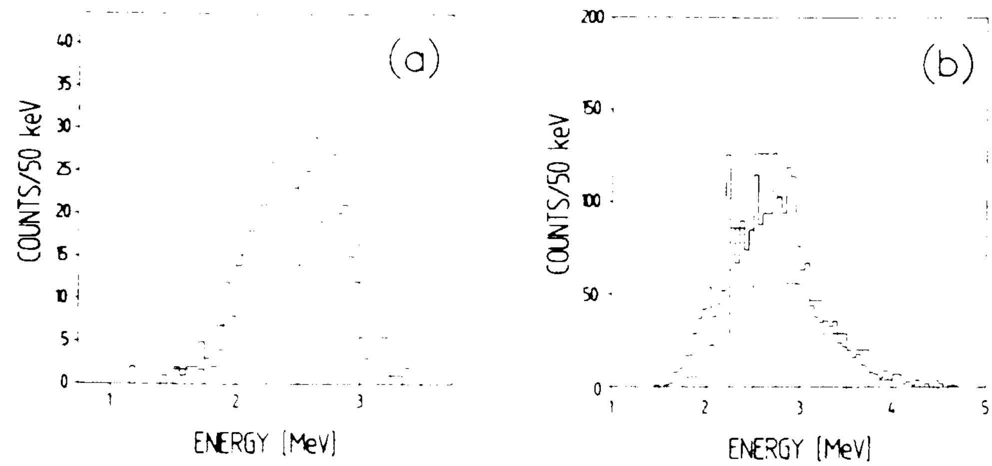


Figure 6: *Energy spectra of $\beta$-delayed protons from the decay of $^{102}$In (a) and $^{100}$In (b). The experimental spectra (solid-line histogram) are compared to predictions (dashed-line histogram) calculated by using a shell-model GT strength together with a statistical model.*

In concluding this section, I would like to mention that the resonance-like GT distribution of $\beta$ decay below $^{100}$Sn may lead to unusually high $\beta$p branching ratios. For the case of $^{101}$Sn, for example, a value close to 40% has been predicted [52]. At the ISOL facility of GSI, $\beta$p measurements have been initiated [54] in order to clarify whether the overproduction predicted for light molybdenum and ruthenium isotopes by rp-process calculations [13] would be altered by unexpectedly high $\beta$p branching ratios.

# 6 Summary and Outlook

In this paper, I have shown that complete $\beta$-decay spectroscopy of very neutron-deficient nuclei has become possible by using beam-line spectrometers. The term "complete" refers to the fact that both $\beta$-delayed protons and $\gamma$-rays were observed, that the normalization of the decay branching ratios was achieved by counting decays and decaying atoms, and that the decay half-lifes were measured with high precision. In this context, I would like to underline in particular the advantage of the ion-counting technique for obtaining *absolute* decay branching ratios. A further experiment of this kind will be devoted to $^{40}$Ti [55]. This nuclide, a member of the

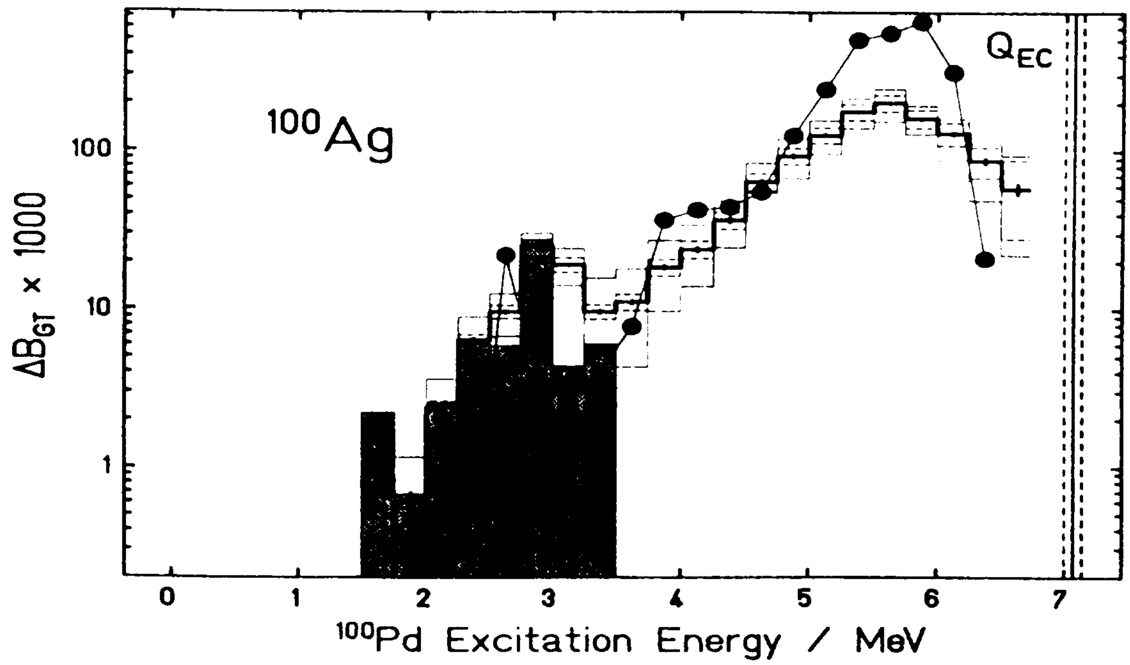


Figure 7: *GT strength per 250 keV interval, determined for the decay of $^{100}Ag$ by using a total-absorption $\gamma$-ray spectrometer (solid histogram). Vertical bars denote the statistical uncertainties. The systematical uncertainties shown by the dotted histograms consist of contributions from the uncertainty of the $Q_{EC}$ value and from the uncertainty in the decay pattern of the daughter nucleus, $^{100}Pd$. The full histogram displays results from a high-resolution study, and the smooth line connecting full circles represents the result of a shell-model calculation for $^{98}Ag$. The experimental $Q_{EC}$ value of $^{100}Ag$ is indicated as a vertical line with the uncertainty given as dashed lines.*

T=2 series as $^{36}$Ca, is of interest since its $\beta$ decay represents the mirror transition to neutrino capture in $^{40}$Ar and is thus relevant to the calibration of the solar-neutrino detector ICARUS.

The study of proton-, $\alpha$, cluster and $\beta$ decay near $^{100}$Sn, which has been described in this report, is a continuing programme, too. Its success depends crucially upon the development of new or refined experimental methods. In the case of ISOL experiments, this includes (i) the development of rapid, efficient and chemically selective ion sources, which involves, e. g., laser resonance ionization or ionization of molecules, (ii) the application of total-absorption $\gamma$-ray spectroscopy, and (iii) the search for cluster decay. In the case of intermediate-energy or relativistic heavy-ion experiments, performed by means of beam-line spectrometers, the recently obtained intensities of $^{100}$Sn have been sufficently high to allow for an unambigious in-flight isotope identification and even for a measurement of gross decay properties. To date, the $^{101}$Sn rate obtained by using fusion-evaporation reactions at the GSI ISOL is one to two orders of magnitude higher than that reached by nuclear fragmentation at GANIL and GSI, respectively. The measurement of the atomic mass of $^{100}$Sn, performed by using [37] $^{58}$Ni($^{50}$Cr,2p6n) fusion–evaporation reactions, seems to support this conclusion. On the other hand, there are apparent improvements possible for the high–energy facilities, such as the increase of the primary beam intensity.

In summary, interesting new results, that are of relevance to nuclear physics as well as astrophysics, have recently been obtained for very proton–rich nuclei in the sd–shell and in the $^{100}$Sn region, and there is every reason to believe that there is more to come along this line soon. Last not least, this optimistic view is also based on the considerable recent progress made in studying such nuclei by other methods such as in–beam $\gamma$ spectroscopy or determination of nuclear radii from relativistic interaction cross–section [56].

# References


[1] E. Roeckl, Rep. Progr. Phys. **55** (1992) 1661.

[2] Proc. Int. Conf. on Exotic Nuclei and Atomic Masses (ENAM95), Arles, 1995, eds. M. de Saint Simon and O. Sorlin, (Editions Frontières, Gif sur Yvette), in print.

[3] G. Audi and A.H. Wapstra, Nucl. Phys. **A565** (1993) 1.

[4] I. Hamamoto and H. Sagawa, Phys. Rev. **C48** (1993) R960.

[5] B. A. Brown, Nucl. Phys. **A577** (1994) 13c.

[6] G. Golò *et al.*, Phys. Rev. **C52** (1995) R1175.

[7] J. Schaffer *et al.*, Z. Phys. **A350** (1994) 91.

[8] J. Dobaczewski and W. Nazarewicz, Phys. Rev. **C51** (1995) R1070.

[9] 1986–1987 Atomic Mass Predictions, ed. G. E. Haustein, At. Data and Nucl. Data Tables, **39** (1988) 185.

[10] R. Davis *et al.*, Phys. Rev. Lett. **20** (1968) 1205.

[11] A. E. Champagne and M. Wiescher, Rev. Nucl. Part. Sci. **42** (1992) 39.

[12] L. Van Wormer *et al.*, Astrophys. J. **432** (1994) 326.

[13] M. Hencheck *et al.*, submitted for publication in Astrophys. J. (1995).

[14] E. Roeckl, in Proc. 2nd Int. Symposium on Heavy Ion Physics and Its Applications (II SHIPA), Lanzhou, 1995 (World Scientific, Singapure), in print.

[15] A. Piechaczek *et al.*, Nucl. Phys. **A584** (1995) 509.

[16] B. A. Brown and B.H. Wildenthal, At. Data Nucl. Data Tables **33** (1985) 347.

[17] W. Trinder *et al.*, Phys. Lett. **B348** (1995) 331.

[18] P. M. Endt, Nucl. Phys. **A521** (1990) 1.

[19] A. Garcia *et al.*, Phys. Rev. **C51** (1995) 3487.

[20] J. Äystö *et al.*, Phys. Rev. **C23** (1981) 879.

[21] E. G. Adelberger *et al.*, Phys. Rev. Lett. **67** (1991) 3658.

[22] W. Trinder *et al.*, Phys. Lett. **B349** (1995) 267.

[23] B. H. Wildenthal and W. Chung in *Mesons in Nuclei*, Vol. 2, eds. M. Rho and D.H. Wilkinson (North-Holland, Amsterdam, 1979).

[24] G. Walter, in Proc. Int. Conf. on Exotic Nuclei and Atomic Masses (ENAM95), Arles, 1995, eds. M. de Saint Simon and O. Sorlin (Editions Frontières, Gif sur Yvette), in print.
[25] B. A. Brown, Phys. Rev. Lett. **69** (1992) 1034.
[26] A. Garcia *et al.*, Phys. Rev. Lett. **67** (1991) 3654, A. Garcia, Ph.D. thesis, University of Washington, 1991.
[27] J. Rapaport *et al.*, Phys. Rev. Lett. **47** (1980) 1518.
[28] D.P. Wells *et al.*, Bull. Am. Phys. Soc. **37** (1992) 1296, M.B. Aufderheide *et al.*, Phys. Rev. **C49** (1994) 678.
[29] P. Magnus *et al.*, Phys. Rev. **C51** (1995) 2806.
[30] C. Iliadis *et al.*, Phys. Rev. **C48** (1992) R1479.
[31] A. Garcia *et al.*, Phys. Rev. **C51** (1995) R439.
[32] J. N. Bahcall, *Neutrino Astrophysics* (Cambridge University Press, Cambridge, 1986), p. 198.
[33] J. N. Bahcall and B. R. Holstein, Phys. Rev. **C33** (1986) 2121.
[34] P. Möller *et al.*, At. Data and Nucl. Data Tables **59** (1995) 185.
[35] R. Schneider *et al.*, Z. Phys. **A348** (1994) 241; J. Friese, in Proc. Int. Nuclear Physics Conf. (INPC'95), Beijing, 1995 (World Scientific, Singapure), in print.
[36] M. Lewitowitz *et al.*, Phys. Lett. **B332** (1994) 20; K. Rykaczewski *et al.*, Phys. Rev. C, in print.
[37] W. Mittig, in Proc. Int. Nuclear Physics Conf. (INPC'95), Beijing, 1995 (World Scientific, Singapure), in print.
[38] K. Schmidt *et al.*, Z. Phys. **A350** (1994) 99.
[39] Z. Janas *et al.*, Phys. Scr. **T56** (1995) 262.
[40] R. J. Tighe *et al.*, Phys. Rev. **C49** (1994) R 2871.
[41] A. Guglielmetti *et al.*, Phys. Rev. **C52** (1995) 740.
[42] Z. Janas *et al.*, to be published.
[43] H. Keller *et al.*, Z. Phys. **A340** (1991) 363.
[44] E. Roeckl, Alpha Decay, in *Nuclear Decay Modes*, ed. D. N. Poenaru (IOP, Bristol), in print.
[45] S. Hofmann, Proton Radioactivity, in *Nuclear Decay Modes*, ed. D. N. Poenaru (IOP, Bristol), in print.
[46] R. D. Page *et al.*, Phys. Rev. Lett. 72 (1994) 1798.
[47] A. Plochocki *et al.*, Z. Phys. **A342** (1992) 43.
[48] M. Pfützner *et al.*, Nucl. Phys. **A581** (1995) 205.
[49] J. Szerypo *et al.*, Nucl. Phys. **A584** (1995) 221.
[50] J. Szerypo *et al.*, to be published.
[51] L. Batist *et al.*, Z. Phys. **A351** (1995) 149.
[52] B. A. Brown and K. Rykaczewski, Phys. Rev. **C50** (1994) 2270.
[53] B. A. Brown and B. H. Wildenthal, Nucl. Phys. **A474** (1987) 290.
[54] R. N. Boyd *et al.*, Proposal for the GSI Experiment U134 (1994), unpublished.
[55] E. Roeckl *et al.*, Proposal for the GSI Experiment S176 (1995), unpublished.
[56] L. Chulkov *et al.*, submitted for publication in Z. Phys. **A** (1995), and to be published.